

Contributions to the discussion of this paper are invited; they should be typewritten and should reach the Secretary, The Royal Institution of Naval Architects, 10 Upper Belgrave Street, London, S.W.1. not later than February 21, 1969.

The Institution is not, as a body, responsible for the statements made nor the opinions expressed by individual authors.

A Theoretical and Experimental Study of the Wavemaking of Hovercraft of Arbitrary Planform and Angle of Yaw

by J. T. Everest, B.Sc. (Eng.)* (Associate-Member)
and N. Hogben, B.Sc., Ph.D.* (Associate-Member)

SUMMARY: In papers by Newman and Poole, and also Barratt (Refs. 1 and 2), systematic calculations of the wave drag of unyawed rectangular and elliptical hovercraft are presented. In work by the present authors (Refs. 3 and 4), it is shown that these calculations agree reasonably well with experiment. This paper extends the earlier work to include arbitrary planforms and angles of yaw.

A method is described using line source elements to calculate both the free wave patterns and the corresponding wave drags for arbitrary unsymmetrical planforms at any angle of yaw. A computer program has been written in which the cushion is defined by the co-ordinates of points suitably disposed round the periphery; the yaw angle can be varied without re-defining the planform. The results of systematic calculations are presented, and comparisons are made with experimental measurements of wave drag, obtained using two hovercraft models. General confirmation of the wave drag theory was obtained, although some evidence of non-linear behaviour was found at low Froude numbers for heavily laden, yawed craft. For Froude numbers in the region of hump speed, theory predicts a very large rate of change of wave drag with yaw angle, and this has been confirmed by experiment. This factor is significant with regard to low speed instability in roll and yaw.

Free wave elevations in the wave pattern have been calculated, including wave profiles under the cushion. In the neighbourhood of the craft some difficulties arise due to transient terms, but it is shown that considerations of surface continuity can help to deal with them. These estimates offer a basis for predicting areas of water contact which is particularly useful for the complicated wave pattern produced by a yawed hovercraft. By an analysis of such wave elevations it has been possible to estimate the wave induced sideforce acting on a yawed craft. For the chosen condition (at hump speed, and with 30° of yaw), the sideforce was found to be over 50% of the wave drag.

INTRODUCTION

The systematic computations of wave resistance in Refs. 1 and 2 have considerable practical value since it has been shown (Refs. 3 and 4), that they agree reasonably well with experiment. These calculations however cover only the wave resistance of symmetrical rectangular and elliptical planforms. In some recent research in Ship Division, the need has been felt to widen the scope of theoretical predictions so that arbitrary unsymmetrical planforms can be handled and so that the corresponding wave patterns can also be computed. The interest in asymmetry grew mainly from the wish to investigate yaw effects. The importance of wave patterns arose in connection with the study of wave interference between the sidewall and the cushion of an immersed sidewall hovercraft. Similar studies of catamaran and trimaran configurations without a cushion had already yielded some useful results (Ref. 7). After explaining briefly the basic theory used, the paper describes the research carried out under three main headings, namely:-

- A. Computation of Wave Resistance
- B. Computation of Wave Elevations
- C. Correlation with Experimental Results

ANALYTICAL BASIS

The analytical basis for this extension of previous computations emerged from work on the general problem of correlating measured wave patterns with corresponding theoretical source

arrays described in Ref. 5. The argument may first be stated for the case of the free waves generated by a travelling symmetrical array of point sources (the free waves are those which carry the energy and would continue to propagate if the source were suddenly removed). It will then be explained how a hovercraft cushion of arbitrary planform can be represented by an array of horizontal line sources which in turn can be constructed by integrating point source distributions. Some discussion of the so-called transient waves is also included (the transient waves do not carry energy and so do not affect the resistance; they are only significant in the neighbourhood of the source and would disappear if the source were removed).

A system of coordinates travelling with the array is used, with the origin at the still water level on the tank centreline; the x, y and z axes are respectively longitudinal, transverse and vertical, with z positive downwards. On this basis, the surface elevation in the pattern of free waves, in a deep tank of breadth b, behind an array of sources of strengths $m_r(x_r, y_r, z_r)$ symmetrical about the tank centreplane, moving at speed V, is given by (see Appendix I):-

$$\zeta_s = \frac{8\pi}{bV} \sum_{n=-\infty}^{\infty} \sum_r m_r \{ A_r \cos \alpha_n x + B_r \sin \alpha_n x \} \cos \beta_n y \quad (1)$$

where

$$A_r = \frac{e^{-z_r(\alpha_n^2/K)}}{(2 - \frac{K^2}{\alpha_n^2})} \cos \alpha_n x_r \cos \beta_n y_r$$

* Ship Division, National Physical Laboratory.

$$B_r = \frac{e^{-z_r(\alpha_n^2/K)}}{\left(2 - \frac{K^2}{\alpha_n^2}\right)} \sin \alpha_n x_r \cos \beta_n y_r$$

$$K = \frac{g}{V^2}$$

$$\alpha_n = K \sec \theta_n$$

$$\beta_n = K \sin \theta_n \sec^2 \theta_n = 2\pi n/b$$

θ_n = Angle between direction of wave propagation and tank centreplane of nth wave component.

Equation (1) can be cast in the general form describing symmetrical free wave modes in a deep tank (Refs. 8 or 9), thus:

$$\zeta_m = \frac{1}{2} \sum_{n=-\infty}^{\infty} a_n \{ \sin \epsilon_n \cos \alpha_n x + \cos \epsilon_n \sin \alpha_n x \} \cos \beta_n y \quad (2)$$

and the coefficients $a_n \sin \epsilon_n$ and $a_n \cos \epsilon_n$ in this equation may be expressed in terms of source strengths and can in fact also be determined by analysis of measured wave patterns (Refs. 8 or 9). Comparing coefficients in Equations (1) and (2) leads to a system of equations relating m_r , a_n and ϵ_n thus:-

$$\begin{aligned} a_n \sin \epsilon_n &= \frac{16\pi}{bV} \sum_r m_r A_r \\ a_n \cos \epsilon_n &= \frac{16\pi}{bV} \sum_r m_r B_r \end{aligned} \quad (3)$$

When the amplitudes a_n are known either from measurement or from Equation (3), the corresponding wave resistance R_w can be calculated from (see Ref. 8 or 9):-

$$R_w = \frac{\rho g b}{16} \sum_{n=-\infty}^{\infty} (2 - \cos^2 \theta_n) a_n^2 \quad (4)$$

with $a_n = a_{-n}$.

To explain the application of the foregoing to hovercraft, it is only necessary to define the relation between source density σ and cushion pressure P_c . From consideration of the component of flux normal to the water surface, this relation may be written approximately (see Ref. 10) as:-

$$4 \pi \sigma = V \frac{\partial \zeta}{\partial x} = \frac{V}{\rho g} \frac{\partial P_c}{\partial x} \quad (5)$$

This equation states that the source density is proportional to the pressure gradient. This leads to a slight difficulty because in the typical hovercraft situation, $\frac{\partial P_c}{\partial x} \rightarrow 0$ everywhere except round the edge (excluding parts parallel to the x axis) where $\frac{\partial P_c}{\partial x} \rightarrow \infty$. This difficulty can be overcome however by noting that the edge can be represented by line sources of density σ_r such that:-

$$\frac{\sigma_r}{V} = \int \frac{\sigma_r}{V} dx = \frac{1}{4\pi\rho g} \int \frac{\partial P_c}{\partial x} dx = \frac{P_c}{4\pi\rho g}$$

where P_c is the pressure assumed uniform within the perimeter and the integration with respect to x is taken across the edge.

The basic components from which a cushion may be constructed are thus elementary horizontal lines of uniform source density arrayed round the perimeter. In most practical cases, a satisfactory representation can be constructed from a relatively small number of straight elements each defined by source density, position of midpoint and inclination to tank centreplane.

It can be shown (see Appendix II), that for the case of an array of such line sources at angle ϕ to the centreplane, the Equations (3) become:-

$$\begin{aligned} a_n \sin \epsilon_n &= \frac{16\pi}{bV} \sum_r \sigma_r' F_r A_r \\ a_n \cos \epsilon_n &= \frac{16\pi}{bV} \sum_r \sigma_r' G_r B_r \end{aligned} \quad (6)$$

where:-

$$\begin{aligned} F_r &= \frac{1}{\cos \alpha_n x_r} \left\{ \frac{\sin [\frac{1}{2}(\alpha_n A + \beta_n) \delta y_r] \cos (\alpha_n x_r + \beta_n y_r)}{(\alpha_n A + \beta_n)} \right. \\ &\quad \left. + \frac{\sin [\frac{1}{2}(\alpha_n A - \beta_n) \delta y_r] \cos (\alpha_n x_r - \beta_n y_r)}{(\alpha_n A - \beta_n)} \right\} \\ G_r &= \frac{1}{\sin \alpha_n x_r} \left\{ \frac{\sin [\frac{1}{2}(\alpha_n A + \beta_n) \delta y_r] \sin (\alpha_n x_r + \beta_n y_r)}{(\alpha_n A + \beta_n)} \right. \\ &\quad \left. + \frac{\sin [\frac{1}{2}(\alpha_n A - \beta_n) \delta y_r] \sin (\alpha_n x_r - \beta_n y_r)}{(\alpha_n A - \beta_n)} \right\} \end{aligned} \quad (7)$$

$$A = \cot \phi$$

$$\delta y_r \operatorname{Cosec} \phi = \text{length of line source } \sigma_r'$$

$$\frac{\sigma_r'}{V} = \frac{P_c}{4\pi\rho g}$$

In all the analysis so far, the source arrays are arbitrary except for a requirement of symmetry about the tank centreplane. This symmetry restriction can be circumvented by the following artifice. If an unsymmetrical array is required, it is placed at a large distance to one side of the centreplane in a very wide tank with a dummy image array at the same distance on the other side. The pair of arrays thus defined is symmetrical, but if the separation is sufficiently large, each half can be treated for practical purposes as a single unsymmetrical array. If the tank width is sufficiently large the open water case is effectively represented.

The computer program used in the present work is based on the foregoing analysis. For convenience however, the input has been arranged so that any arbitrary planform may be defined in terms of the coordinates of a series of points suitably disposed round the perimeter. The computer then joins these points with straight line source elements. It will also apply any desired angle of yaw without the need to re-define the coordinates. The output given is the wave resistance and the wave amplitudes and phases which can be used in Equation (2) to compute the elevations in the free wave pattern. The so-called local or transient disturbance is not included, and for many practical purposes this is not important. There are however occasions when it is important and an approximate method for predicting some of the effects of the transient terms at the cushion perimeter has been developed; the basis

of this method is explained in Section B(b). The possibility of including more exact computations of the transient effects in the program is being explored.

A. COMPUTATION OF WAVE RESISTANCE

(a) Comparison with known results

The program was checked successfully against two-dimensional theory (Ref. 13), and subsequently against the results for a rectangular planform in open water (Refs. 1 and 2). Good agreement was achieved in the three-dimensional case by using a large tank width to approximate to open water, and limiting the number of terms in the summation to about one hundred. The wave drag of a rectangular hovercraft ($L/B = 1.5$) running in a tank of width $10B$ is shown in Fig. 1, in comparison with the result of Barratt (Ref. 2). In cases where the cushion perimeter is curved and it is not possible to represent it by a limited number of straight lines, a good approximation can be obtained using a large number of elementary line sources.

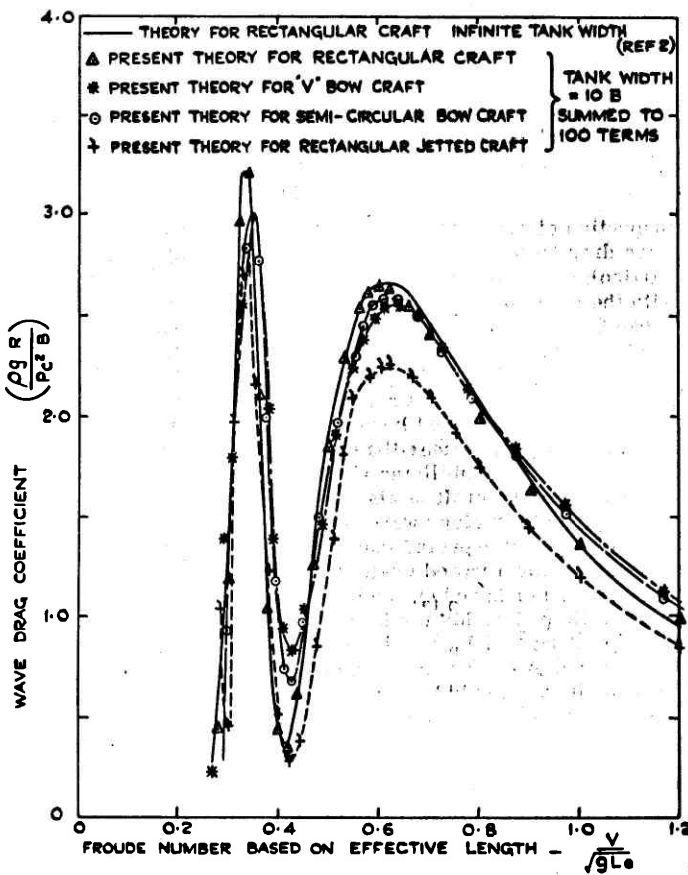


Fig. 1. Wave drag of rectangular, 'V' bow and semi-circular bow hovercraft

$$L_e/B = 3/2; L_e = \frac{\text{(Cushion Area)}}{\text{(Maximum Beam)}}$$

For example, calculations have been made in which a circle was represented by 72 elementary line sources. Comparison with the exact solution of Barratt for this case is seen to be good (Fig. 2), although small discrepancies are introduced at low Froude number. Undoubtedly the correlation would have improved had the number of line sources been increased. Bearing in mind the restrictions of linear theory at the lower

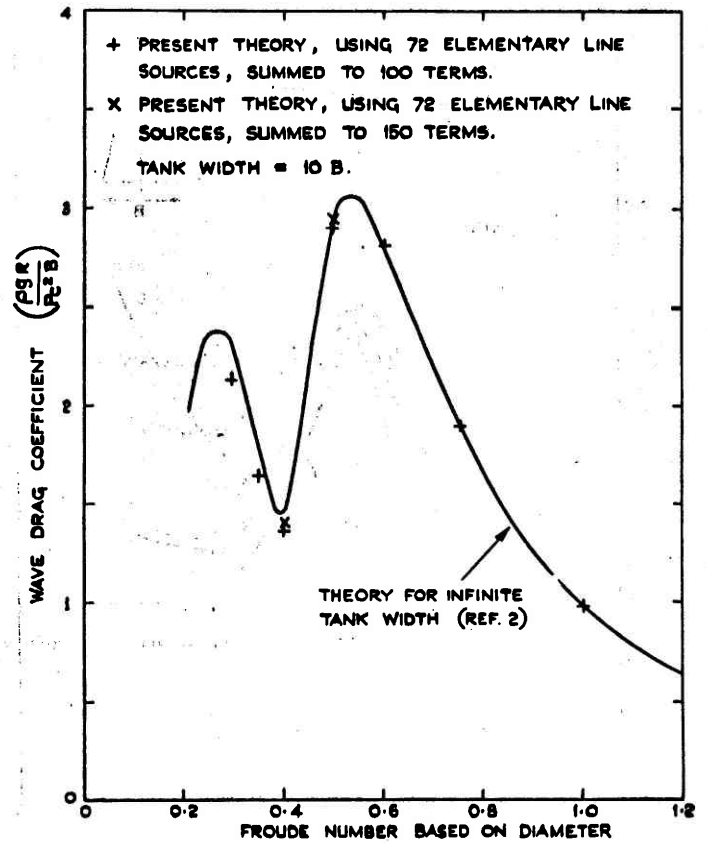


Fig. 2. Wave drag of circular hovercraft

Froude numbers (Ref. 4), the increased computation time associated with increasing the number of sources was not thought to be justified.

(b) Simple Geometrical Planforms

In the absence of alternative prediction methods, it has been the general practice in the past to use theoretical results for rectangular craft to estimate the wave drag of craft having more complicated planforms. For these purposes, an 'effective' cushion length (L_e) was employed, defined as cushion area divided by cushion beam, in place of the overall cushion length. This change affects both length/beam ratio and Froude number.

It is now possible to represent arbitrary planforms using elementary line sources. Results obtained from craft having semi-circular and 'V' bow forms ($L_e/B = 1.5$) are illustrated in Fig. 1 in comparison with results for a rectangular planform of the same aspect ratio. As might be expected from the somewhat arbitrary definition of Froude number, there are certain differences in phase in comparison with a rectangular planform of the same effective aspect ratio, but otherwise the curves are very similar, and tend to justify the simplified approach used in the past. This result implies a relative insensitivity of wave drag to planform design in the unyawed condition.

The results of further studies in which the wave drag of unyawed triangular planforms was calculated, are shown in Fig. 3. As with rectangular planforms, there is a tendency for the larger length/beam craft to have a reduced non-dimensional wave drag, with hump speeds tending to occur at higher Froude numbers. There was little evidence of an optimum angle of entrance, unless very fine bows could be considered. These would clearly have practical disadvantages.

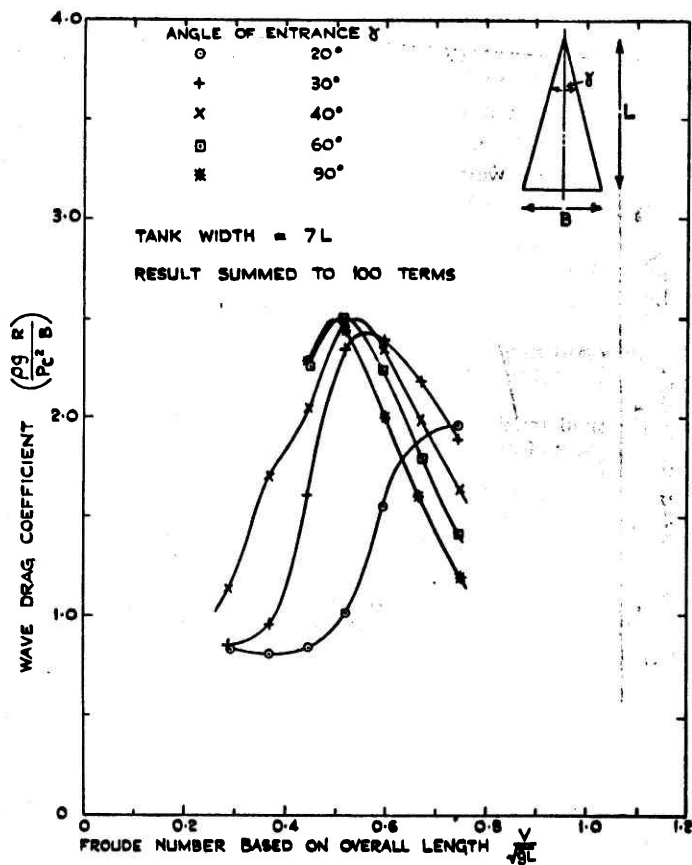


Fig. 3. Wave drag of triangular craft

(c) Pressure Variations over the Cushion

It is quite simple to represent a pressure variation over the planform by using further line sources to approximate to pressure contour lines. Unfortunately, not a great deal is known at present of such pressure distributions, although it should be possible to obtain an approximation if wave profiles under the craft were known. These approximations could be estimated or measured, possibly by operating a hovercraft statically over a solid representation of the wave surface.

For illustration, the wave drag of a rectangular craft fitted with peripheral and stability jets has been calculated. For the exercise, it was decided to use pressure distributions obtained experimentally with the craft hovering over a smooth solid surface. This is clearly an approximation, but it was not convenient to obtain a better representation of the pressure field. Results are illustrated in Fig. 1. Although it was assumed that the pressure field was felt beyond the confines of the craft, it was considered more appropriate to non-dimensionalise wave resistance and speed in terms of the jet centreline dimensions.

It is evident that the crude representation of the stability jets did result in an appreciable deviation from the basic theory, but this investigation has not been pursued further because, since the development of skirts, jet effects are no longer so important.

Pressure variations in the cushion associated with compartmentation for purposes of stability, and also cushion air cross flow, are important present day influences. In particular, the out-flow of cushion air along wave troughs will induce considerable changes in the pressure field, with direct influence on both craft stability and wavemaking effects. The calculation of wave patterns under the craft is discussed in subsection B(b).

(d) The Yawed Condition

Application of the method to a hovercraft running at yaw has been possible by adding an image cushion to satisfy the symmetry requirement. If a wide separation is chosen between the craft and its image, no wave interference will occur, and the solution for the single yawed craft can be effectively determined.

(i) Rectangular Planform

A rectangular planform was chosen for initial study. This offered relative simplicity of analysis, while being suitable for subsequent experimental determination of wave drag using the model described in Ref. 4. The hovercraft ($L/B = 3/2$) and its image were assumed to be running at a separation of $4L$ in a tank of width $8L$. Consideration of the angle at which waves propagate away from a body suggests that for separations in excess of a model length the wave interference effects will be small. This has been verified experimentally in Ref. 7, (see also Fig. 7). The choice of $4L$ was basically one of convenience, in the knowledge that mutual interference between the craft would not occur. Yaw angles in the range 0° - 90° were considered for $0.4 < F_n < 1.4$. The estimated wave drags, which have been halved to exclude the image craft, are presented in Fig. 4. The notation has been adopted that Froude number is based on actual cushion length (between jet centrelines), and that the non-dimensional wave drag is based upon actual cushion beam, irrespective of yaw angle (see diagram on Fig. 4). Allowing for this notation it is seen that for yaw angles of 0° and 90° , the results agree with Ref. 2. By symmetry, at these angles the rate of change of wave drag with yaw angle must be zero.

Inspection of the plotting demonstrates a very rapid rise in wave drag with angle of yaw in the range 10 - 30° . The effect is particularly severe for Froude numbers in the range 0.40 - 0.50 , with the wave drag rising by a factor of 8.8 for $F_n = 0.40$, between 0 and 45° of yaw. Undoubtedly this dramatic rise in wave drag at low speeds has a bearing on the stability losses which have been experienced by yawed craft. A number of factors may be involved but the wave elevations round the periphery are specially significant because water contact of the skirts on local wave peaks near the bow will cause nose down pitching moments and de-stabilising yaw moments. The surface deformation under the craft is also important because cross flow and escape of air along wave troughs will cause loss of stiffness. It is to be expected that both these effects will be most pronounced for a yawed craft at speeds close to the hump Froude number based on the beam dimension. For a length/beam ratio of 1.5 , this would lead to a critical Froude number based on length of $F_n = 0.45$; this suggestion is supported by experience. A craft travelling in this critical speed range, and rotating in yaw would be tending to produce a wave system around it which was rapidly changing and steepening. A factor of almost 9 on wave drag would suggest wave heights increasing by a factor of 3 . It is therefore quite possible that the waves would grow under the craft at a rate greater than the craft's natural response, especially if the craft had a low pitch/roll stiffness.

The greatest significance of this investigation is obviously in the region of hump speed. However, it is interesting to note that at Froude numbers in excess of 0.9 , yaw has only a small influence on wave drag. Reference to Fig. 4 illustrates that there is a slight advantage to be gained in wave drag when travelling at yaw at high speed, although it seems almost certain that practical considerations would tend to rule out this technique, unless severe cross winds were being experienced.

(ii) Realistic Planform—H.D.2

The cushion planform of the craft was determined by marking around the perimeter of the inflated skirts of a suitable model, when hovering over ground. This approach has advantages over working exclusively from drawings, although small variations will almost certainly occur when moving at speed over

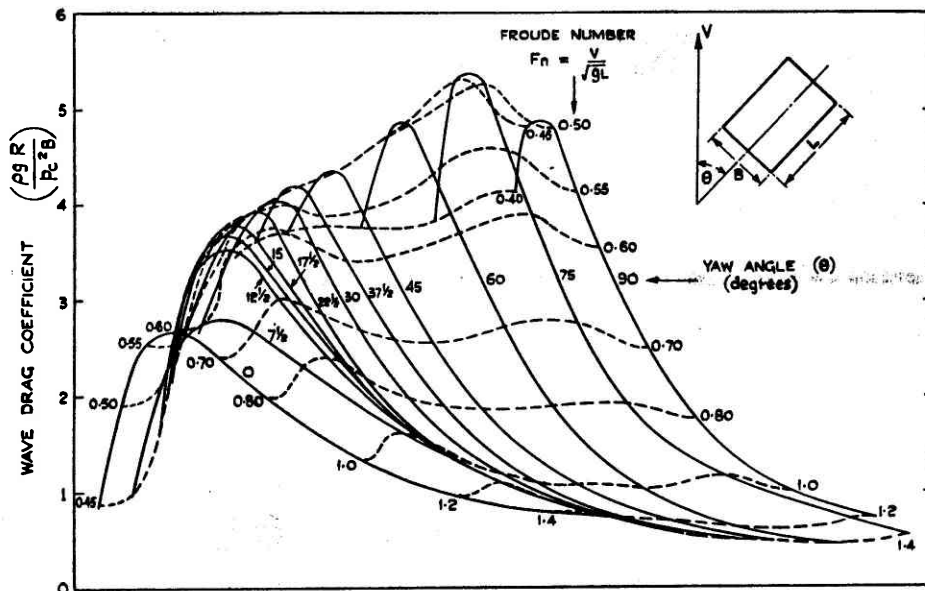


Fig. 4(i). Variation of wave drag in deep water with Froude number and yaw angle. Rectangular planform, $L/B = 3/2$

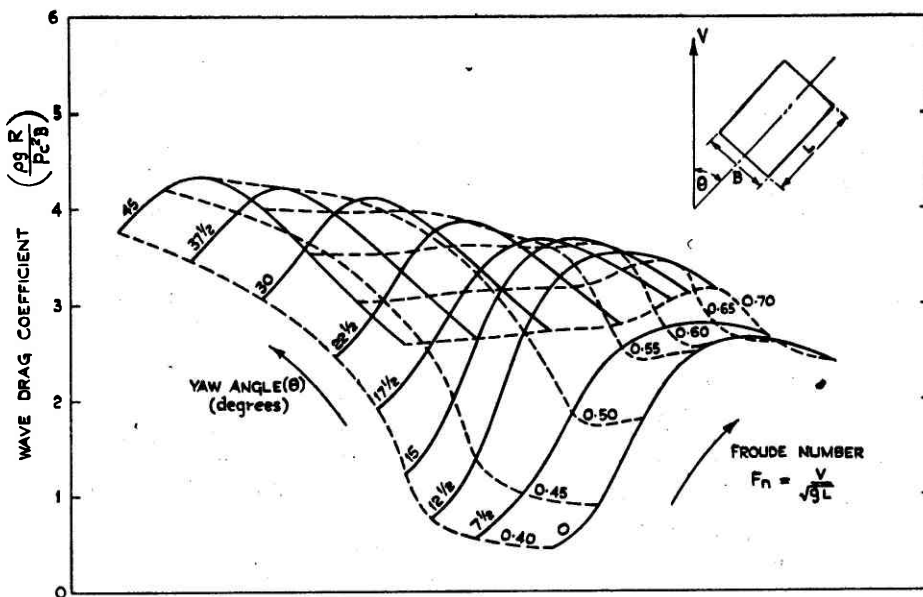


Fig. 4(ii). Variation of wave drag in deep water with Froude number and yaw angle. Rectangular planform, $L/B = 3/2$

water. As with the unskirted craft, it is unlikely that the area upon which the cushion pressure is reacted will be precisely that defined geometrically, since cushion air outflow will have some effect upon the water surface. These influences will be exaggerated where wavemaking is significant, due to peaks and troughs in the wave system.

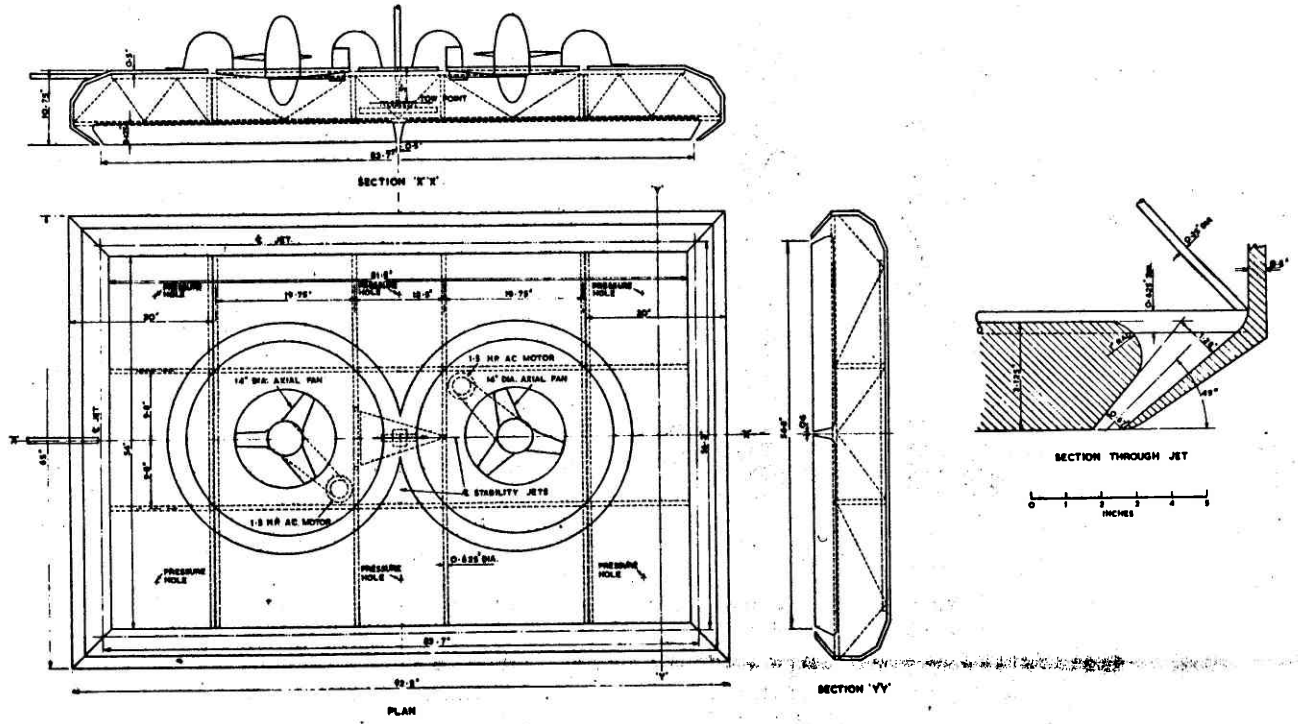
The model particulars are summarised in Fig. 5; the effective length/beam ratio (L_e/B) was 1.65. Wave drag was estimated assuming a separation of $4L_e$ between the model and its image, and a tank width of $8L_e$. Yaw angles between 0 and 90° were considered over a range of Froude numbers between 0.4 and 1.4. The estimated wave drags, which have been halved to exclude the image craft are shown in Fig. 6, non-dimensionalised in terms of the effective length (L_e) and the maximum beam (B).

At zero yaw angle, the results compare closely with estimates made for a rectangular craft having the same effective length/beam ratio. As in the earlier work, a rapid rate of change of wave drag with yaw angle is found for Froude numbers in the range 0.40-0.55. This effect is most severe for the range of yaw angles between 10 and 30°.

B. COMPUTATIONS OF WAVE ELEVATIONS

(a) Free Wave Elevations around a Hovercraft

The computer program described in Section A completely determines the free wave system. This means that the wave pattern behind the craft, clear of the transient effects, can be mapped by the computer in very great detail (see Fig. 7). Even



N.B. FRAMES SHOWN IN BROWN LINES



Fig. 5(i). General arrangement of free hovercraft model

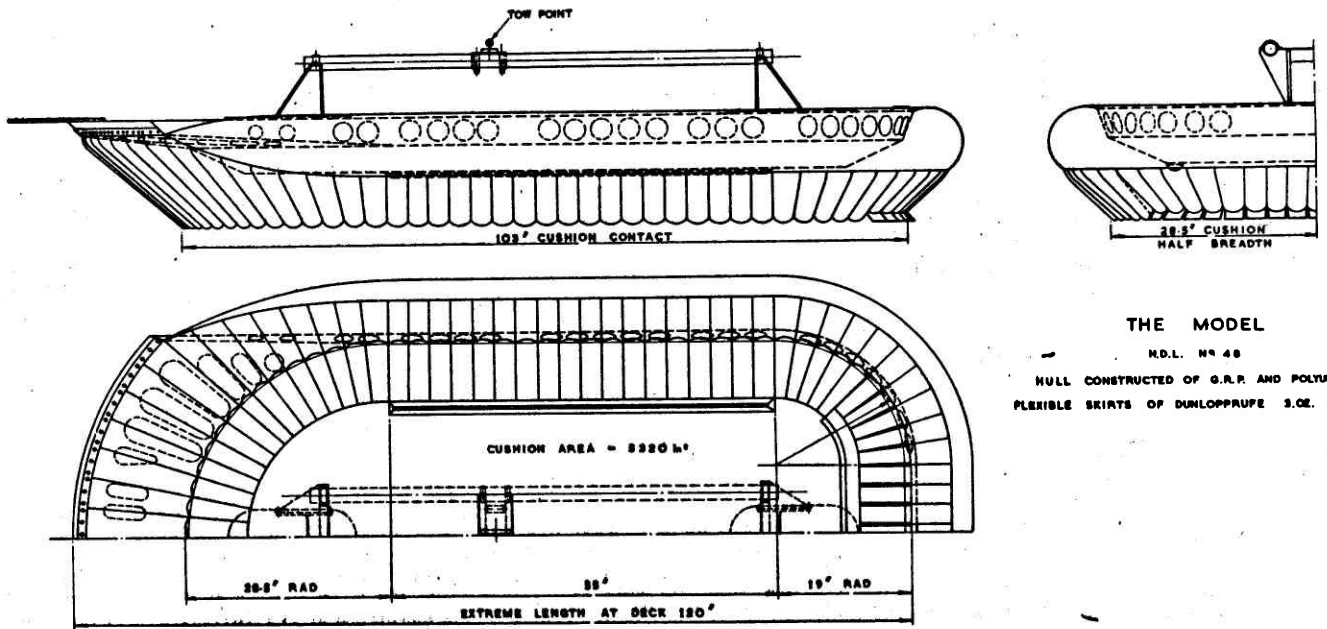


Fig. 5(ii).

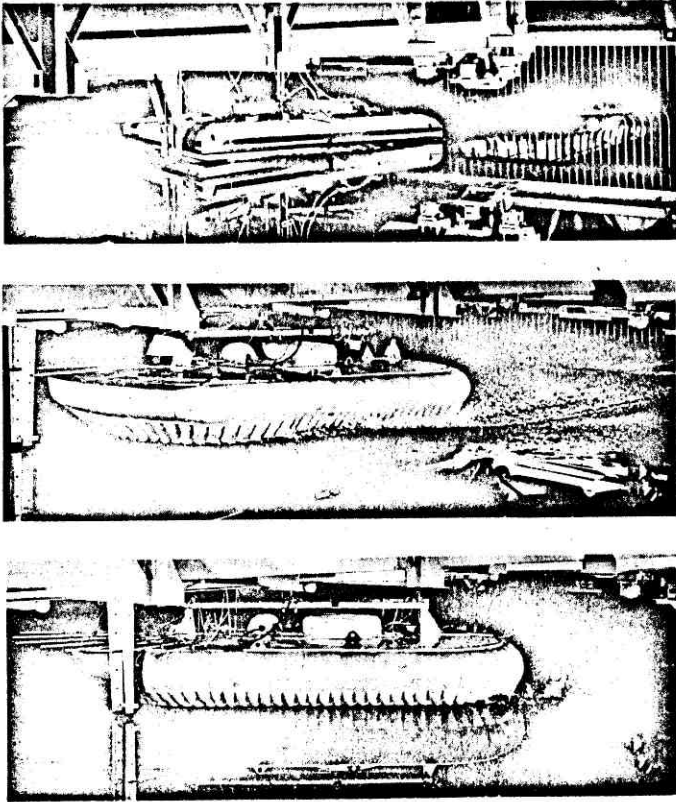


Fig. 5(iii). The models running in No. 3 tank, Feltham

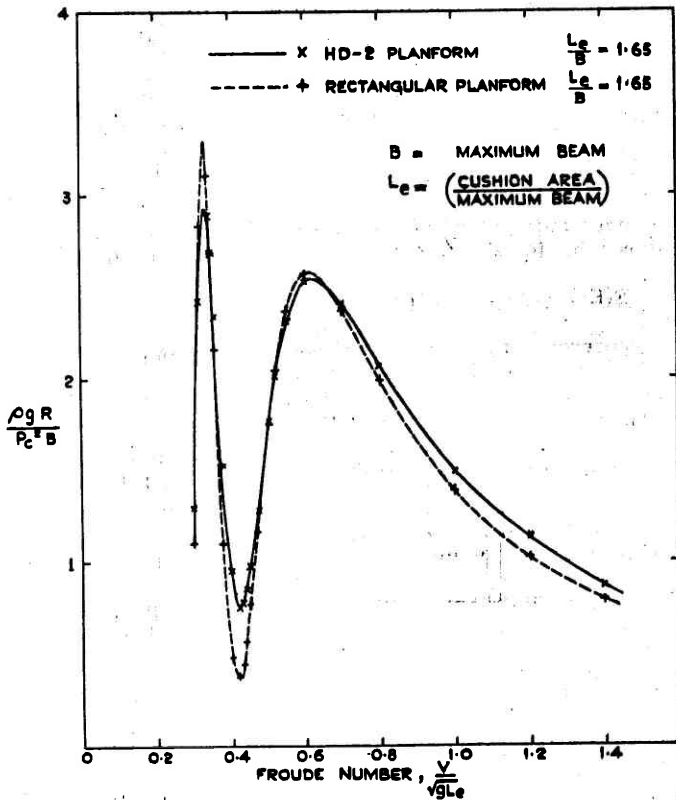


Fig. 6(i). Variation of wave drag in deep water with Froude number; zero yaw angle

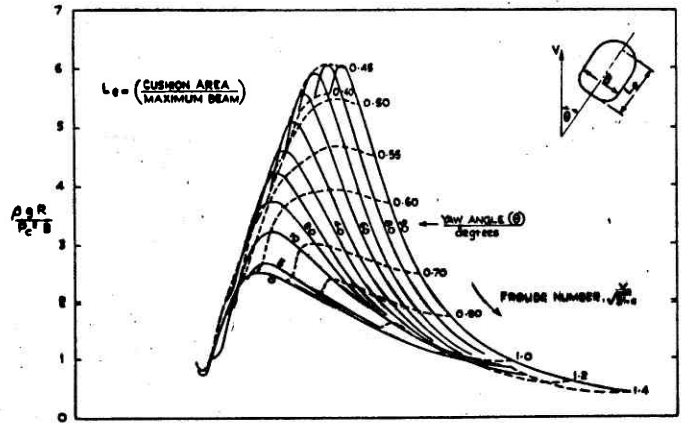


Fig. 6(ii). Variation of wave drag in deep water with Froude number and yaw angle. HD-2 planform, $L_e/B = 1.65$

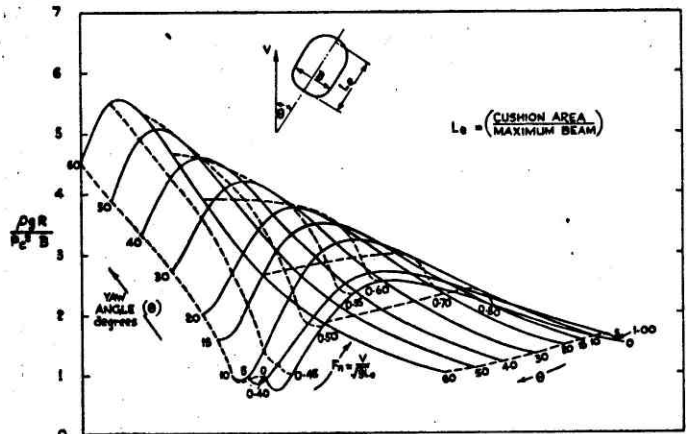


Fig. 6(iii). Variation of wave drag in deep water with Froude number and yaw angle. HD-2 planform, $L_e/B = 1.65$

under the cushion, mapping of the free waves gives an approximation to the water surface shape which may be adequate for many practical purposes (see Fig. 8). In some cases, however, greater accuracy is required. When estimating the extent of skirt contact, for example, wave elevations predicted in this way could be misleading.

There are two important points to be noted when computing wave elevations in the neighbourhood of the cushion. The first of these is that the free waves, as predicted by the computer for a source element, contain a dummy system extending ahead so that the whole pattern is symmetrical about the source. In many cases, these artificial dummy wave components can be removed. In the unyawed case, for example, there is little difficulty because only the forward skirt contributes free waves within the cushion. For a yawed craft, however, dummy free waves from all parts of the skirt, and especially the sides, can encroach on the cushion and are difficult to remove. This trouble can be overcome by the laborious process of using short elementary line sources instead of the maximum length of line source available from geometrical considerations, and suppressing the corresponding dummy waves.

The second point to be noted is that under the cushion the influence of the transient waves is important. The computer program is not yet able to include these. As described in the

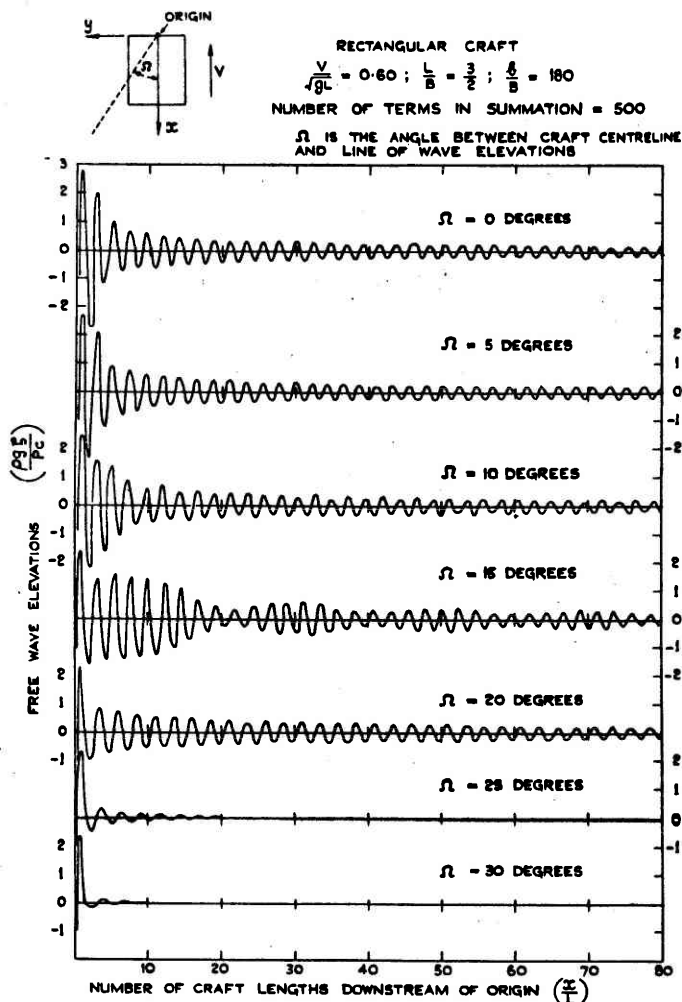


Fig. 7. Free wave elevations at large distances from the craft along lines radiating from the origin ($V/\sqrt{gL} = 0.60$)

next section, however, for certain specific cases their magnitude can be reasonably well estimated by examining the two-dimensional solutions and invoking a condition of surface continuity to interpret the three-dimensional situation.

(b) Transient Wave Elevations

A complete solution for the wavemaking of a two-dimensional pressure field including transient terms is given by Lamb (Ref. 13). The total wave elevation is composed of three components, namely, the oscillatory free wave elevation, an exponential term (E), and a constant term dependent on the local free surface pressure. (Upstream of the pressure field, the free wave term and the constant term have zero amplitude). Summarising the results of Lamb for a pressure field extending from $0 \leq x \leq \infty$,

$$x > 0, \zeta = \frac{P_c}{\rho g L} [2\pi \cos(kx) - E(Kx) - \pi]$$

$$x < 0, \zeta = \frac{P_c}{\rho g L} E(-Kx)$$

where $E(Kx) = [\pi/2 - Si(Kx)] \cos Kx + Ci(Kx) \sin(Kx)$, and $K = g/V^2$.

This surface deformation is illustrated in Fig. 9. It may be noted that the water surface is continuous for $x = 0$, in spite of

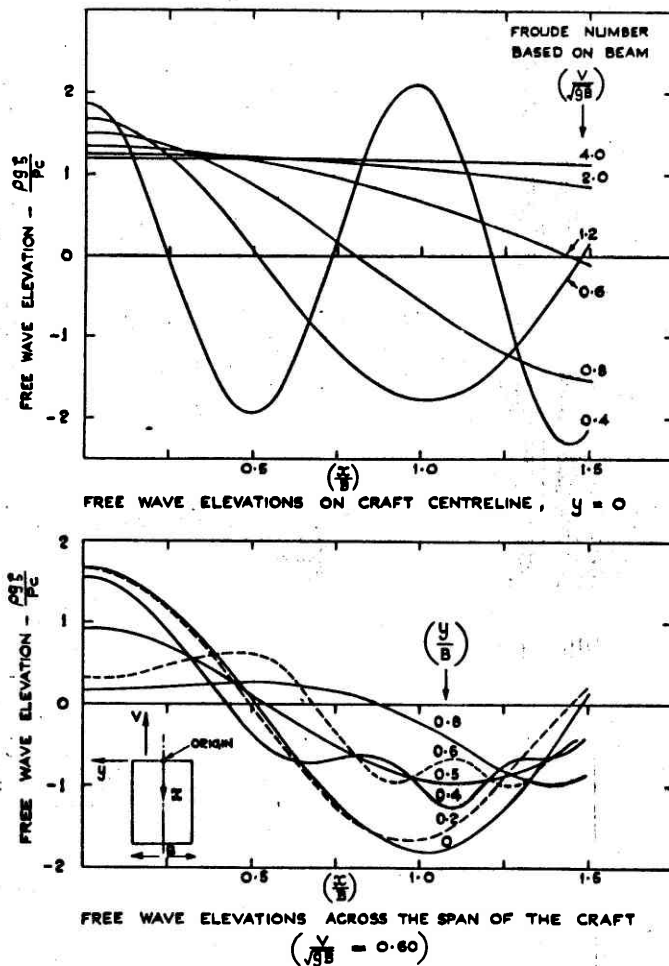


Fig. 8. Free wave elevations under rectangular craft at zero yaw angle

the fact that the gradient becomes infinite at this position. It follows that for $x = 0$,

$$E(Kx) = \frac{1}{2} [2\pi \cos(Kx) - \pi] = \pi/2$$

To represent a two-dimensional hovercraft, similar wave elevations of the opposite sign are added at the after end of the cushion. The wave drag is defined as the horizontal component of the pressure force integrated over the distribution (see Ref. 16).

$$\text{Thus } R_w = \iint_S P_c(xy) \cdot \frac{dz}{dx} \cdot dx \, dy = \iint_S P_c(xy) \, dy \, dz$$

where S is the area of water surface covered by the pressure $P_c(xy)$ and S' is the projection of S on to the yz plane.

For the two-dimensional case

$$R_w = \frac{W}{L} [\zeta_{x=0} - \zeta_{x=L}] = \frac{W}{L} \cdot \frac{2P_c}{\rho g} \cdot [1 - \cos\left(\frac{1}{Fn^2}\right)]$$

For large but finite beam/length ratios we may put $B = \frac{W}{P_c L}$ hence

$$\frac{\rho g R_w}{P_c^2 B} = 2 \left[1 - \cos\left(\frac{1}{Fn^2}\right) \right]$$

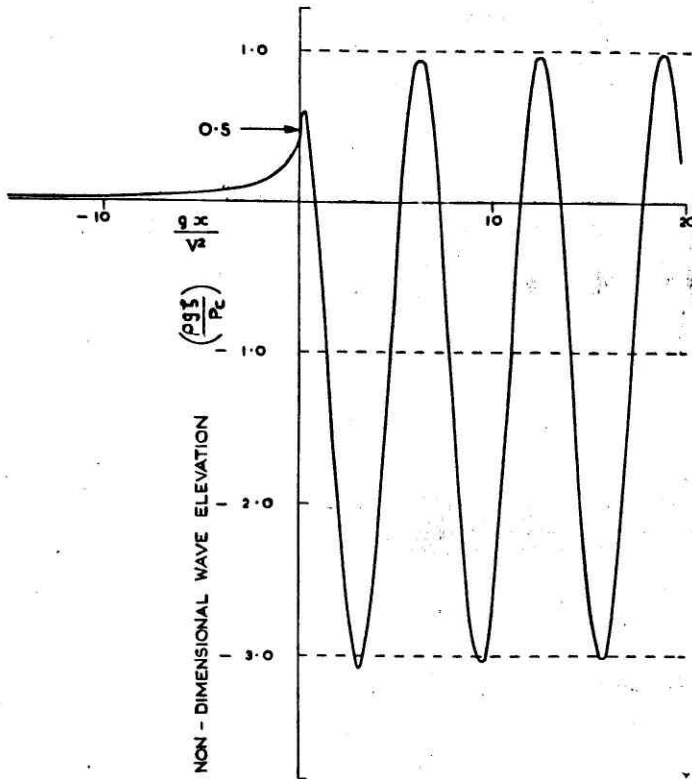


Fig. 9. Wave profile generated by a uniform pressure extending from $x = 0 \rightarrow x = \infty$. Two-dimensional theory

It should be noted that the wave drag does not depend upon the transient terms, $E(KL)$.

For three-dimensional conditions, a solution is considerably more difficult. However, it is possible to deduce certain of its properties from the solution of the free wave system, discussed earlier, and the condition of surface continuity. For finite pressure loadings, water passing into a zone of modified pressure must always have a continuous surface, although its gradient may be infinite. Also, linear free waves cannot exist upstream of their source, although this comment does not apply to transient waves.

Consider a line source at $x = 0$, having a length B normal to its direction of motion, across which the pressure rises by P_c . The free wave component is readily estimated using the theory described in this note and the cushion pressure displacement term is straightforward. Assuming the transient waves to be symmetrical upstream and downstream, it follows that for conditions along the line source (i.e. $x = 0$) we may write

Transient wave elevation = $\frac{1}{2}$ [Free wave elevation less the static cushion depression]

as for the two-dimensional case above.

Using this relationship, estimates have been made of the transient waves for $x = 0$. The non-dimensionalised elevations, which are functions of Froude number based on source length, and ratio of source length to tank width only, are presented in Fig. 10. Some slight approximation was introduced due to a limitation in the number of terms in the free wave estimate. This is the probable cause of the oscillation in the estimated transient wave elevation along the line source. Note the rapid fall in the elevations towards the ends of the line source, and also the sensitivity to Froude number. The two-dimensional solution is seen to agree with this three-dimensional result at zero Froude number. Unfortunately, the approach cannot be used where x does not equal zero.

The sides of a rectangular pressure field produce no waves, but the effects of the transient waves from the leading and trailing edges will be significant as the ends of the craft are approached. It is of note that for an unyawed rectangular craft, the wave elevations at bow and stern determine the theoretical wave drag. Due to symmetry, transient terms do not appear in the final solution, and the wave drag can be calculated from the difference of the average free wave elevations at bow and stern. Similar conclusions will apply to any unyawed symmetrical craft. It also seems very probable that drag and sideforce could be estimated for non-symmetrical yawed craft from free wave elevations, without regard to the transient wave pattern.

(c) Wave Induced Sideforce

An estimate of sideforce has been made for the case of a rectangular craft, yawed at 30° and running at a Froude number of 0.6. Each of the sides of the craft was divided into seven line sources in order to attempt to avoid the effects of the dummy wave system mentioned earlier. Undoubtedly a finer sub-division would have produced more precise results, but the computation time would have risen sharply. Free wave elevations along the edges of the craft, calculated in this manner, are illustrated in Fig. 11. Considerable asymmetry is evident in the wave pattern, and in spite of the fact that transient waves are not included, it would be reasonable to suggest from inspection that water contact would occur along the side marked AD and also along AB adjacent to the point B (see diagram on Fig. 11). Experimental evidence confirms these conclusions.

An approximation to the wave induced sideforce was obtained using the relation

$$\text{Sideforce} = \iint_S P_c(xy) \cdot \frac{dz}{dy} \cdot dx \cdot dy = \iint_{S''} P_c(xy) \cdot dx \cdot dz$$

where S is the area of the water surface covered by the pressure $P_c(xy)$ and S'' is the projection of S on to the xz plane.

An indication of the accuracy of this procedure was achieved by comparing the drag force calculated using a similar expression (as described in the preceding section) with precise estimates of wave drag. If the effect of dummy waves could be completely suppressed, the two results would be equal. For the trial condition, a 22% discrepancy was found, which must be regarded as significant; the error would be reduced if a greater number of line sources were used. For this case, the wave induced sideforce was estimated to be 52% of the estimated wave drag. Although considerable sideforces had been measured earlier on yawed hovercraft, it had been assumed that the force was produced in large measure by skirt contact effects. Further studies are in hand to extend knowledge of these lateral forces.

C. EXPERIMENTAL RESULTS

In an earlier paper (Ref. 4), the results of wave pattern measurements made on a rectangular hovercraft model were described. Some results of these experiments, which were for an unyawed condition, are shown in Fig. 12. Good agreement was found with theoretical results, although a certain degree of scatter was found around hump speed. Accuracy was shown to improve at high speeds where water surface gradients were lower. This study has been extended to include yawed conditions for which the theory has now been developed.

(a) Yawed Rectangle

The construction of this model is described in Ref. 4, (see also Fig. 5). It was unskirted, having peripheral jets inclined at 45° to the horizontal, and vertical stability jets on the fore and aft, and transverse centrelines. The model was free to rise, trim and roll, but was constrained in yaw. Test were conducted in the No. 3 tank NPL Feitham, having a cross section of 48 ft.

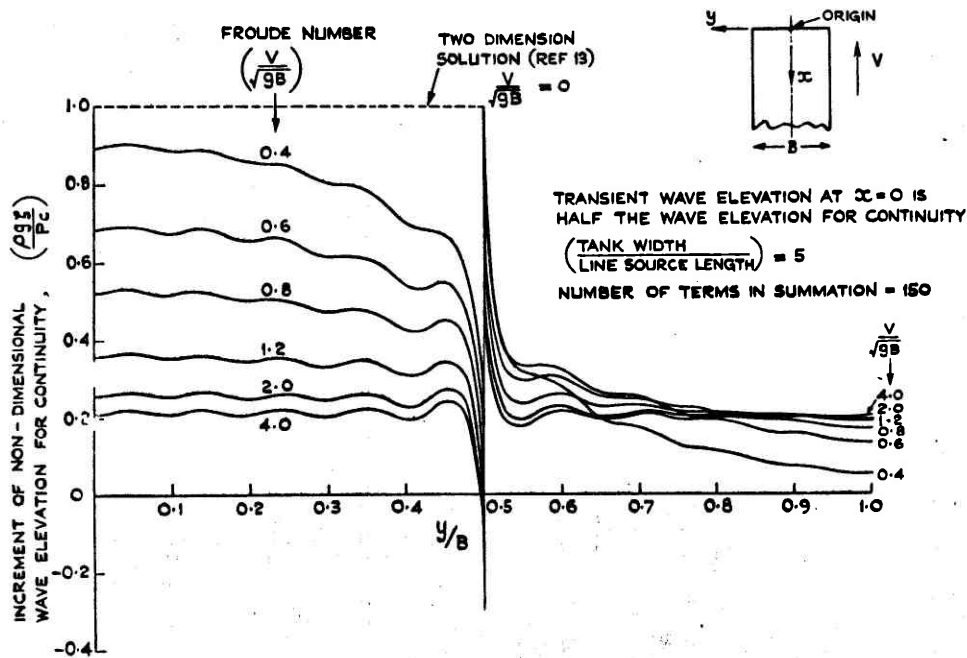


Fig. 10(i). Variation of transient wave elevation along line source at $x = 0$ as a function of Froude number

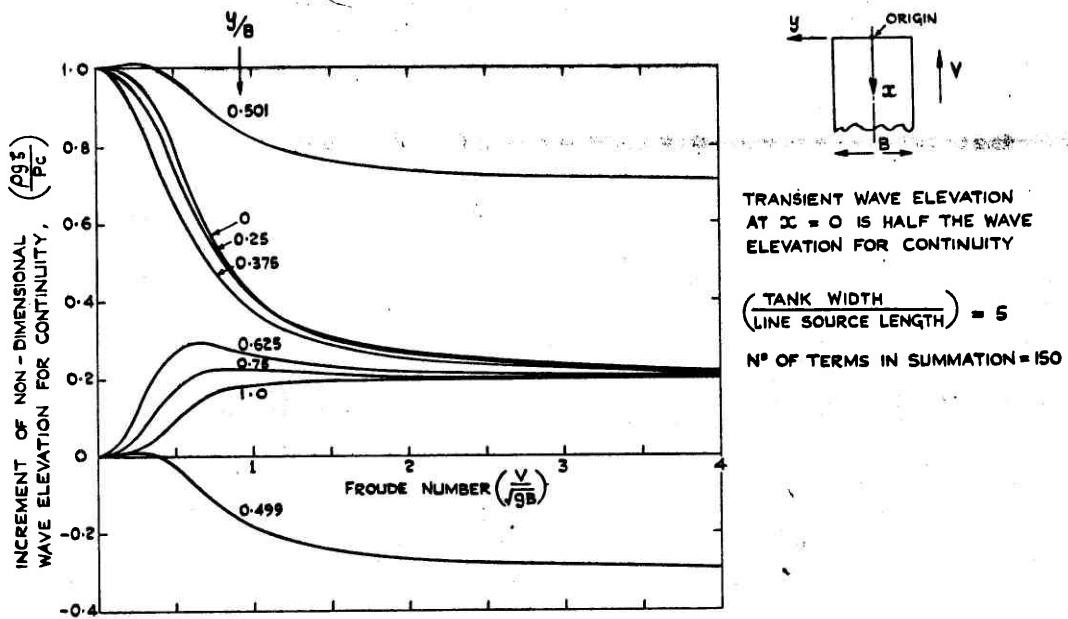


Fig. 10(ii). Variation of transient wave elevation along line source at $x = 0$ as a function of Froude number

wide by 25 ft. deep. At the test speeds this can be regarded hydrodynamically as unrestricted water. Aerodynamic influences from the carriage structure might have some slight effect on model drag and attitude, but earlier work has indicated that the magnitude of the effect on wavemaking at the test speeds can be discounted.

Force and attitude measurements were taken and are reported in Ref. 15. For the purposes of this paper however, the discussion is limited to measurements of wave drag. Wave elevations were measured using manually operated pointers fitted to the carriage across the full tank width (since symmetry about the tank centreline did not exist). These enabled the determination of wave elevations along a pair of transverse cuts across the tank downstream of the model. The Egger's analy-

sis (Refs. 8 and 9) allows the estimation of the wave energy contained in an unsymmetrical wave pattern, but unfortunately the computer program available only considered symmetrical patterns. To overcome this difficulty, an image wave pattern was introduced in such a manner that one of the tank walls could be taken to be a plane of symmetry for purposes of analysis. The distance of the transverse cuts from the model was chosen such as to avoid any wave reflection from the tank wall which might have complicated the procedure. The wave drag of the yawed model was thus half that of the model and its image; a result which was readily computed.

Some slight variation of weight was necessary to trim the model out of water contact which developed at the bow at quite small yaw angles. It is unlikely however that this would

●●● EXPERIMENTAL POINTS DETERMINED FROM WAVE PATTERN MEASUREMENTS.

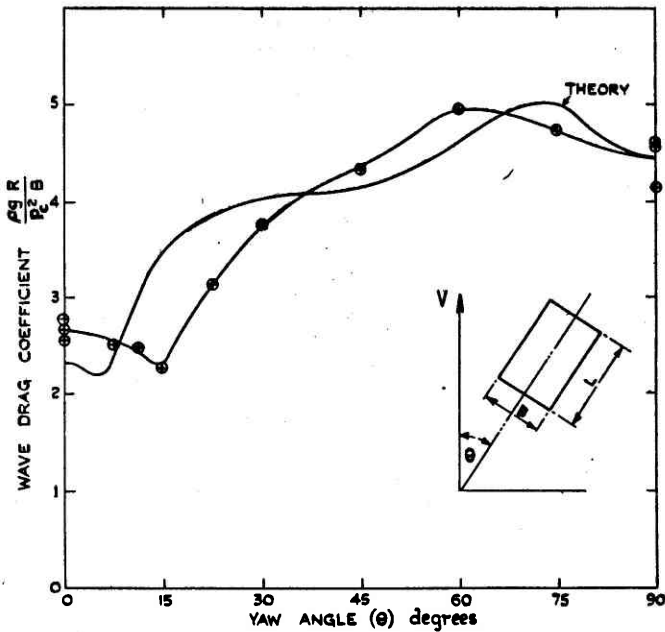


Fig. 13(i). Comparison of measured and predicted wave drag for rectangular hovercraft at yaw. Froude number $F_n = V/\sqrt{gL} = 0.533$, $L/B = 3/2$

⊕ EXPERIMENTAL POINTS DETERMINED BY WAVE PATTERN MEASUREMENTS.

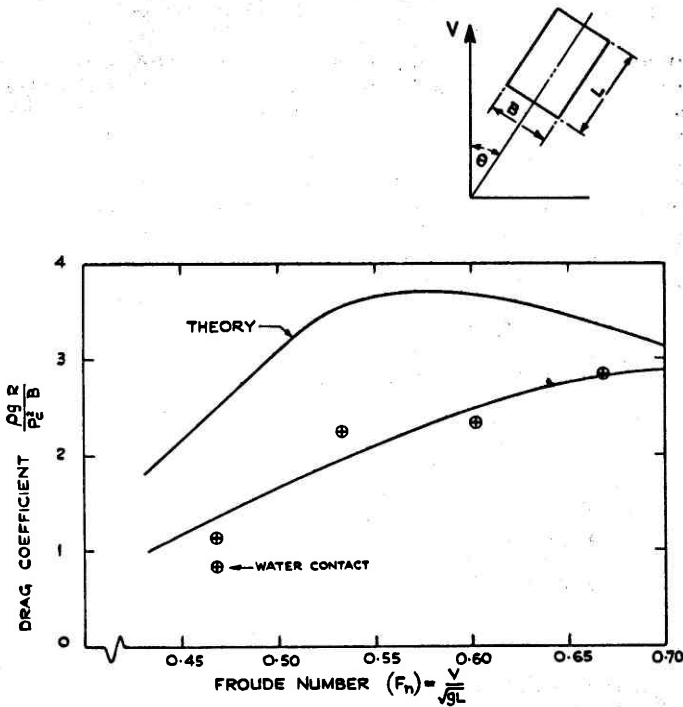


Fig. 13(ii). Comparison of measured and predicted wave drag as a function of Froude number for a rectangular hovercraft at yaw
 $L/B = 3/2$, Yaw angle $\theta = 15^\circ$

length (L) and beam (B) have been assumed to be measured to the peripheral jet centreline, parallel and normal to the craft centreline respectively. The limitations of this assumption are self-evident, and it might be argued that a small increase in these values would be justified when representing the pressure distribution. Unfortunately, no simple formulation is available.

(b) Yawed Model of Realistic Design — H. D. 2.

Tests were made in No. 3 Tank, Feltham as for the rectangular model described above. This discussion will be confined to wave drag measurements, and comment relating to the force and moments acting is reported in Ref. 14. Experiments were made over a Froude number range between 0.4 and 0.8, and two values of the load parameter (P_c/Le) were considered. Tests were made both unyawed, and through a range of yaw angles up to 60° , but with greatest attention being given to a yaw angle of 20° .

Fig. 14(i) compares unyawed wave drag predictions with measurements. The model weight was large during these experiments ($P_c/Le = 1.16$), and it is probable that the slight discrepancies observed were associated with high wave steepnesses in the wave pattern (see also Ref. 16). Some degree of phase difference between the two curves is evident, resulting in a significant over-estimate of wave drag at $F_n = 0.45$. A similar effect was observed for the rectangular model. Subsequent tests with the model yawed at this Froude number have resulted in a general confirmation of this experimental result. The tendency for experiment and theory to diverge even further for large yaw angles is illustrated in Fig. 14(ii).

MEASURED WAVE DRAG

YAW(deg) WEIGHT (lb) FAN (r.p.m.)
+ + 0 333 1580

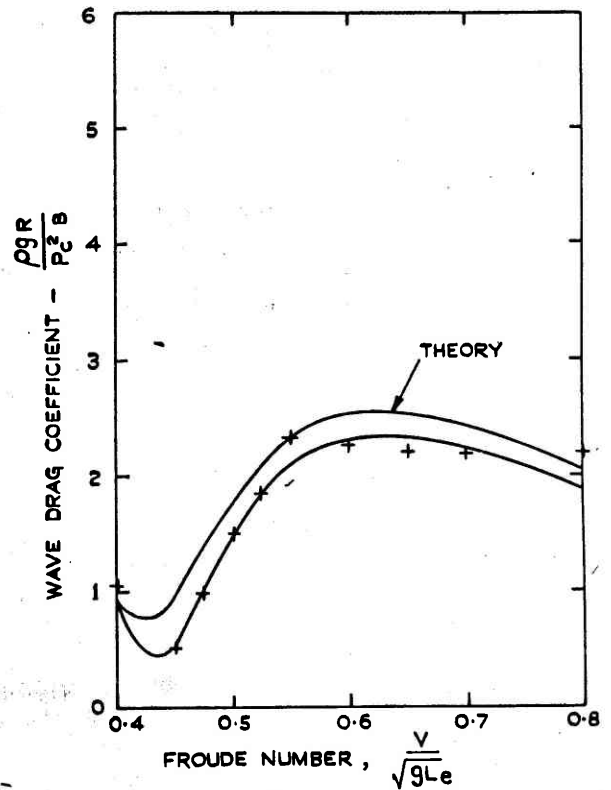


Fig. 14(i). Wave drag as a function of speed

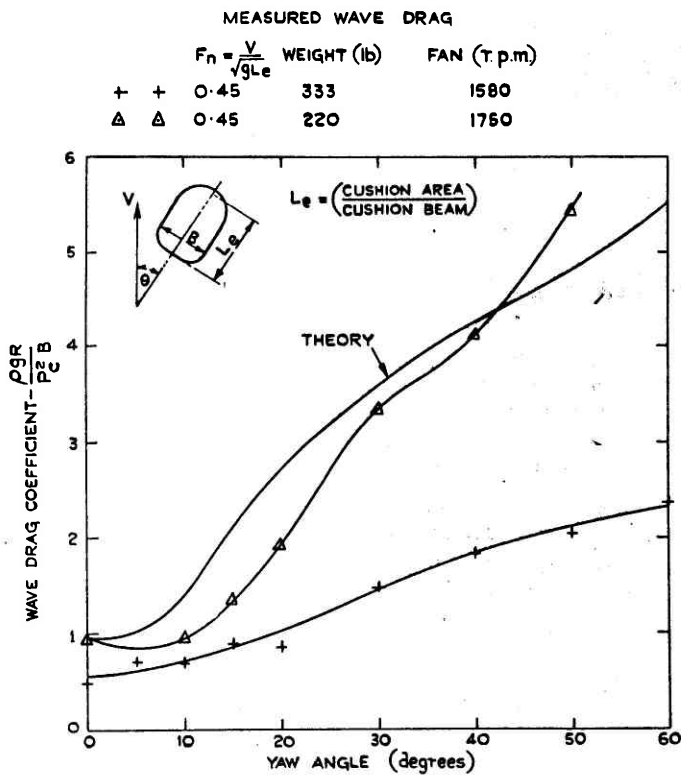


Fig. 14(ii). Wave drag as a function of yaw angle

Considerable wave breakage and skirt contact was observed during these experiments, and it was anticipated that correlation with theory would be poor. In order to minimise these effects, further tests were made in which the craft weight was reduced such that $(P_c/Le) = 0.77$, and the fan speed increased. Significantly better correlation with theory was achieved in this condition, as is evident from Fig. 14(ii). Further tests with the model in its lighter condition were made at 20° of yaw, in the range $0.4 < F_n < 0.7$. The agreement with theory was quite good (see Fig. 14(iii)), although there was a tendency for theory to over-estimate wave drag, more particularly at the lower Froude numbers.

To sum up, although theory appears applicable for lightly laden craft, poor correlation between theoretical and measured wave drag has been observed where air clearances are small, and the craft loading is large, more particularly at the lower Froude numbers and for yawed conditions. Skirted craft can be operated satisfactorily at weights above that at which water contact has become developed, and at which non-skirted craft would experience unacceptable total drag increases. Wave drag can therefore be measured conveniently on skirted craft where it would be impossible upon non-skirted designs. In such conditions, the applicability of the wave theory may be limited, and estimates should be made with care.

CONCLUSIONS

1. A method of estimating the wavemaking resistance of hovercraft of arbitrary planform and pressure distribution has been developed; the method can be applied to craft operating at angles of yaw. Computer programs have been written to simplify the analysis. Agreement with earlier theoretical results for simple planforms has been checked.

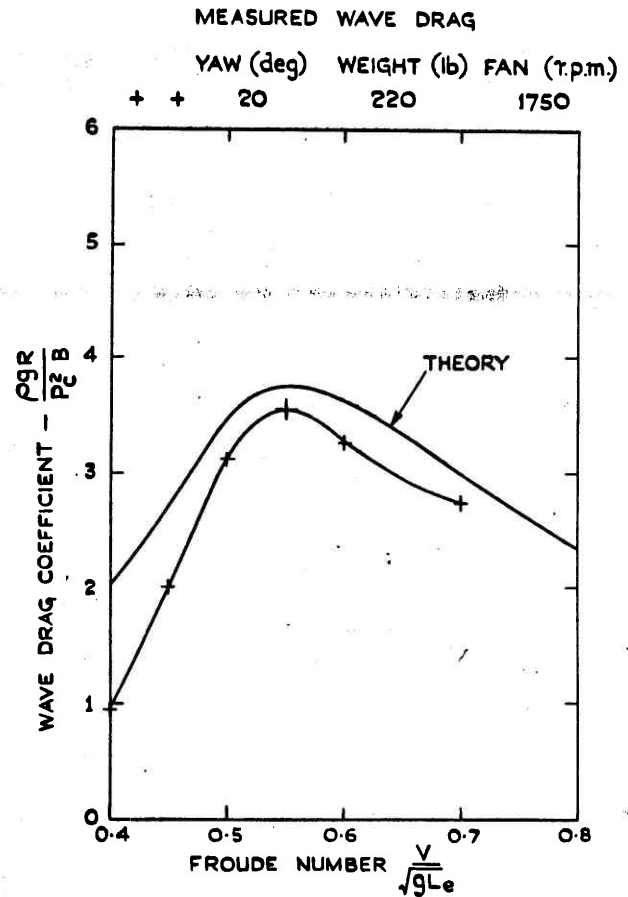


Fig. 14(iii). Wave drag as a function of speed

2. For Froude numbers in the region of hump speed, theory predicts a very large rate of change of wave drag with yaw angle, and this has been confirmed by experiment. This factor is significant with regard to low speed hovercraft instability in roll and yaw.
3. Free wave elevations in the wave pattern have been calculated including profiles under the craft. Near the craft some inaccuracy is introduced if transient terms are omitted. An indication of the magnitude of these is included in the paper.
4. A simple estimate of wavemaking induced sideforce has been made for a yawed hovercraft. For the chosen condition the sideforce was found to be over 50% of the wave drag.
5. General confirmation of the wave drag theory has been obtained during experiments upon two hovercraft models. As expected, some evidence of non-linear behaviour was found at low Froude numbers for heavily laden, yawed craft.

ACKNOWLEDGEMENT

This paper is published by permission of the Director of the National Physical Laboratory. The authors wish to express their appreciation to all members of Ship Division staff who have contributed to this work, especially Mr. R. C. Willis who ran the experiments.

NOMENCLATURE

A	Cot ϕ or as defined in Fig. 11 according to context
A_r	Amplitude function (Equation (1))
a_n	Amplitude of nth wave component
B	Cushion beam or as defined in Fig. 11 according to context
B_r	Amplitude function (Equation (1))
b	Tank width
$E(Kx)$	Function describing transient waves
F_n	Froude number, V/\sqrt{gL}
F_r	A function (Equation (7))
$F(\theta)$	A function of θ (Appendix I)
$f(t)$	A function of t (Appendix I)
G_r	A function (Equation (9))
g	Acceleration due to gravity
I	An integral (Equation (9))
I_b	An integral (Equation (10))
K	Wave number, g/V^2
L	Craft length
L_e	Effective cushion length
m_r	Strength of source r
$m_r(x_r, y_r, z_r)$	m_r at x_r, y_r, z_r
n	Wave component number
P	Pressure
P_c	Cushion pressure
R_w	Wave resistance
S	Area of the water surface covered by the pressure $P_c(xy)$
S'	The projection of S on to the yz plane
S''	The projection of S on to the xz plane
t	A parameter (Equation (11))
V	Craft speed
W	Craft weight
x, y, z	Longitudinal, transverse and vertical co-ordinates respectively
x_r, y_r, z_r	Particular values of x, y, z
α_n	$K \sec \theta_n$
β_n	$K \sin \theta_n \sec^2 \theta_n$
γ	Angle of entrance of triangular hovercraft
$\delta y_r \csc \phi$	Length of line source
ϵ_n	Phase of nth wave component
ζ	Wave elevation
ζ_s, ζ_m	Wave elevations as defined by Equations (1) and (2) respectively
η	Transverse component of distance along line element (Equation (16))
θ	Angle between direction of wave propagation and tank centreline or angle of yaw according to context
θ_n	θ for nth wave component
ρ	Density of water

σ	Source density
σ'	Line source density
σ_r	σ for element r
σ'_r	σ' for element r
ϕ	Angle between line element and tank centreline
Ω	Angle between craft centreline and line of wave elevations (see Fig. 7)

REFERENCES

1. Newman, J.N. and Poole, F.A.P.: 'The Wave Resistance of a Moving Pressure Distribution in a Canal'. Schiffstechnik Vol. 9, No. 45, 1962.
2. Barratt, M.J.: 'The Wave Drag of a Hovercraft'. J.F.M. 22 Part 1, pp. 39-47, 1965.
3. Hogben, N.: 'An Investigation of Hovercraft Wavemaking'. J.R.Ae.S. February, 1966.
4. Everest, J.T. and Hogben, N.: 'Research on Hovercraft over Calm Water'. Trans. RINA, Vol. 109, 1967, p. 311.
5. Hogben, N.: 'A Computer Program for Correlating Measured Wave Patterns with Theoretical Source Arrays'. Ship Div. TM 189, September, 1967.
6. Everest, J.T.: 'Wave Drag of Hovercraft of Arbitrary Planform including the Effects of Running at Angles of Yaw'. Ship Div. TM 170, 1967.
7. Everest, J.T.: 'Some Research on the Hydrodynamics of Catamarans and Multihulled Vessels in Calm Water'. Trans. NECIES, 1968.
8. Eggers, K.: 'Über die Ermittlung des Wellenwiderstandes eines Schiffmodells durch Analyse Seines Wellensystems'. Schiffstechnik Vol. 9, Part 46, p. 79, 1962.
9. Gadd, G.E. and Hogben, N.: 'The Determination of Wave Resistance from Measurements of the Wave Pattern'. Ship Div. Rep. 70, November, 1965.
10. Havelock, T. H.: 'The Theory of Wave Resistance'. Proc. Roy. Soc. A, Vol. 138, 1932.
11. Havelock, T.H.: 'Wave Resistance Theory and its Application to Ship Problems'. Trans. SNAME, Vol. 59, p. 13, 1951.
12. Titchmarsh, E.C.: 'Theory of Fourier Integrals'. Oxford University Press, 1948.
13. Lamb, H.: 'Hydrodynamics'. Cambridge University Press, 6th Edition, 1932.
14. Everest, J.T. and Willis, R.C.: 'Experiments on a Skirted Hovercraft running at Angles of Yaw, with Special Attention to Wave Drag'. Ship Div. Rep. 119, 1968.
15. Everest, J.T. and Willis, R.C.: 'Experiments to Investigate the Wave Drag of a Rectangular Hovercraft running at Angles of Yaw'. Ship Div. TM 204, 1968.
16. Hogben, N.: 'Hovering Craft over Water'. Advances in Hydrosience, Vol. 4, 1968. (Academic Press).

APPENDIX I

Derivation of Equation (1)

From Ref. 11, the free wave pattern for a travelling point source $m_1(0, 0, z_r)$ in open deep water may be defined by the following expression for the surface elevation ζ_1 :-

$$\zeta_1 = \left(\frac{8Km_1}{V} \right) I \quad (8)$$

where

$$I = \int_0^{\pi/2} F(\theta) \cos \alpha x \cos \beta y \, d\theta \quad (9)$$

$$F(\theta) = e^{-(z_1 \alpha^2/K)} \sec^3 \theta$$

$$\alpha = K \sec \theta$$

$$\beta = K \sin \theta \sec^2 \theta$$

In a tank of breadth b , by the method of images, the corresponding result may be obtained by replacing I by I_b written:-

$$\begin{aligned} I_b &= \sum_{n=-\infty}^{\infty} \int_0^{\pi/2} F(\theta) \cos \alpha x \cos \beta (y + nb) \, d\theta \quad (10) \\ &= \sum_{n=-\infty}^{\infty} \int_0^{\pi/2} F(\theta) \cos \alpha x \cos \beta y \cos \beta nb \, d\theta \end{aligned}$$

Writing now:-

$$b\beta = bK \sin \theta \sec^2 \theta = 2\pi t$$

so that

$$d\theta = \frac{2\pi \cos^3 \theta \, dt}{bK (1 + \sin^2 \theta)}$$

I_b becomes:-

$$I_b = \sum_{n=-\infty}^{\infty} \int_0^{\infty} f(t) \cos 2\pi nt \, dt \quad (11)$$

where

$$f(t) = \frac{2\pi}{bK} \frac{F(\theta)}{(2 - \cos^2 \theta)} \cos \alpha x \cos \beta y \cos^3 \theta \quad (12)$$

It can be shown that this expression for $f(t)$ satisfies the conditions for the application of Poisson's formula (Ref. 12), which is:-

$$\sum_{n=-\infty}^{\infty} \int_0^{\infty} f(t) \cos 2\pi nt \, dt = \frac{1}{2} f(0) + \sum_{n=1}^{\infty} f(n) \quad (13)$$

Thus since $f(t)$ is even in this case:-

$$\begin{aligned} I_b &= \frac{1}{2} \sum_{n=-\infty}^{\infty} f(n) \\ &= \frac{\pi}{bK} \sum_{n=-\infty}^{\infty} \frac{F(\theta_n) \cos^3 \theta_n}{(2 - \cos^2 \theta_n)} \cos \alpha_n x \cos \beta_n y \quad (14) \end{aligned}$$

with

$$\beta_n = \frac{2\pi n}{b} = K \sin \theta_n \sec^2 \theta_n$$

Hence:-

$$\zeta_1 = \frac{8\pi}{bV} \sum_{n=-\infty}^{\infty} m_1 \frac{e^{-(z_1 \alpha_n^2/K)}}{(2 - K^2/\alpha_n^2)} \cos \alpha_n x \cos \beta_n y \quad (15)$$

Equation (1) for a symmetrical array of sources may be derived from Equation (15), with appropriate changes of origin and elimination by symmetry of all odd terms in y .

APPENDIX II

Derivation of Equations (6) and (7)

It is assumed that horizontal line source elements are arranged in pairs with centres distant $+y_r$ and $-y_r$ from the centreplane and inclined at an angle ϕ to it. It is also assumed that there is a uniform source density σ'_r along each line and, since it is horizontal, that z_r is constant. Thus along each line:-

$$x = x_r + A\eta \text{ where } A = \cot \phi$$

$$y = y_r + \eta$$

$$z = z_r$$

Hence, Equations (3) may be written for the elements at $+y_r$:-

$$\begin{aligned} a_n \sin \epsilon_n &= \frac{16\pi}{bV} \sum_r \int_{-1/2\delta y_r}^{+1/2\delta y_r} \frac{\sigma'_r e^{-(z_r \alpha_n^2/K)}}{(2 - K^2/\alpha_n^2)} \times \\ &\quad \cos [\alpha_n(x_r + A\eta)] \cos [\beta_n(y_r + \eta)] \, d\eta \\ a_n \sin \epsilon_n &= \frac{16\pi}{bV} \sum_r \int_{-1/2\delta y_r}^{+1/2\delta y_r} \frac{\sigma'_r e^{-(z_r \alpha_n^2/K)}}{(2 - K^2/\alpha_n^2)} \times \\ &\quad \sin [\alpha_n(x_r + A\eta)] \cos [\beta_n(y_r + \eta)] \, d\eta \quad (16) \end{aligned}$$

The expressions for the elements at $-y_r$ which must also be added are identical.

Evaluation of the integrals in Equation (16) leads to the Equations (6) and (7).